Frequency Stability for Distributed Generation Connected through Grid-Tie Inverter

Eric Glover, *Student Member, IEEE,* Chung-Ching Chang, *Student Member, IEEE,*
Dimitry Gorinevsky*, *Fellow, IEEE,* and Sanjay Lall, *Senior Member, IEEE*

***Abstract*—Conventional power generation systems rely on the rotating inertia of large synchronous generators to maintain stability in the power balance and frequency control loops. The increasing penetration of inverter-connected distributed generation proportionally reduces the fraction of conventional stabilized power used in the distribution system. It is an open question whether the primary feedback loop related to frequency control would remain stable as the fraction of the distributed generation increases in a distribution system. We develop and analyze a control model of a grid-connected distribution system to determine the stability in response to disturbances from the grid, such as grid frequency variations. Our conclusion is that for tie-in inverter connection of distributed generation, the transients can remain stable and grid frequency disturbances will not be amplified as long as the inverter controller is well-tuned. This conclusion holds for a broad range of parameter values explored in this work percentage of the distributed generation penetration, power factor of the load, load power, transmission line impedance, LCL filter and PLL in inverter system.**

***Index Terms*—Distributed power generation, Power distribution, Power system stability, Power system control Inverters.**

I. Introduction

THE existing electric grid was designed for generation by centralized, dispatchable power plants. It is expected that more and more of distributed generation will be gradually added to the grid as the use of renewable sources such as rooftop solar panels increases. These sources are connected to the distribution grid through inverters. An inverter converts the DC power from its generation source to AC power that can be fed into the grid. The inverter must control the amount of active power (P) and reactive power (Q) injected into the grid while matching the grid frequency and phase.

The most common type of inverter control system in use in the United States today is the grid-tie system [1]. A grid-tie inverter measures the local grid frequency using a phase-locked loop (PLL) and attempts to output power at this frequency. The inverter also receives an active power setpoint from its generation source. For photovoltaics, this setpoint is often set using a maximum power point tracking algorithm [2]. A simple feedback controller (e.g., a PI) is implemented to adjust the output power until it reaches setpoint. This approach is in compliance with IEEE Standard 1547 [3]. Such grid-tie system is typically connected to the distribution system through an LCL filter as discussed in [4]–[6].

Of specific interest in this paper is how power balance and frequency control are maintained in systems as penetration of inverter-connected generation sources increases. In conventional systems with large synchronous generators, the rotating inertia of these generators provides stability to the system. As penetration of inverter-connected generation increases, the overall inertia of the system decreases. Surprisingly, there appears to be little literature discussing this important issue. In [1], the discussion of control functions for systems with high penetration of photovoltaics does not include the stability of the overall distribution system. In [7], frequency control and stability is discussed for systems with high penetration of wind generation. A system involving energy storage with fuel cells is proposed to provide primary frequency control.

At current low levels of renewable penetration there are few concerns. Distributed generation is connected to the grid through an inverter with a simple control system. However, the question is whether this will continue to work at higher levels of inverter-connected penetration. It is not well understood if the control structure of the distribution system must change to accommodate increasing levels of inverter-connected generation sources. This causes concern for utilities that must guarantee the reliability of the grid. The goal of this paper is to establish from a controls perspective if the power stability can be guaranteed as penetration of inverter-connected generation sources increases. We focus on the stability of a distribution system under varying parameters with an inverter-connected generation source controlled using a grid-tie system.

II. Simulation Model

A simulation was developed in MATLAB/Simulink using the SimPowerSystems toolbox and its component model templates for electric power generation, transmission, distribution, and control, see [8]. Figure 1 shows the high-level diagram of the developed Simulink sim.

The sim details a balanced 3-phase distribution system that receives anywhere from zero to one hundred percent of the load power from an inverter-connected generation source. To simplify the model, the load and the distributed generation are both aggregated. The sim consists of four main elements: the utility grid model, the load model, the inverter model, and the inverter control logic model.

The utility grid has essentially a constant voltage as seen from the distribution grid. However, it may have a varying fre-

* Corresponding author, email: gorin@stanford.edu

E. Glover was with the Department of Electrical Engineering, Stanford University, Stanford, CA 94305, USA. He is now with Sargent and Lundy, Chicago, IL 60603, USA (e-mall: Eric.S.Glover@SargentLundy.com)

C.-C. Chang, D. Gorinevsky, and S. Lall are with the Department of Electrical Engineering, Stanford University, Stanford, CA 94305, USA (e-mall: {bobbyc, gorin, lall}@stanford.edu

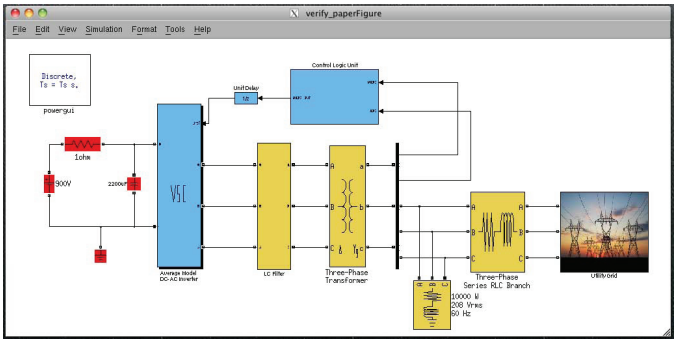

Fig. 1. High-level diagram of SimPowerSystems simulation.

quency. This is built into the model by using the Three-Phase Programmable Voltage Source from the SimPowerSystems toolbox that allows for step and ramp changes in frequency and phase. The utility grid voltage source is connected to the load through a realistic 3-phase distribution line model including the 120kV/25kV substation step-down transformers, a 30km 25kV-line, 25kV/120V distribution transformer, and a distribution line. The load in the simulation is an aggregated model of the load in the full distribution system. The active and reactive power demands of the distribution system can be adjusted by adjusting this load. SimPowerSystems contains models of loads where active power (P) and reactive power (Q) can be explicitly specified. This load is then connected to ground.

The first element of the simulated inverter system is a three bridge DC-AC Inverter model from the SimPowerSystems used to convert a DC voltage source to a 3-phase source. Switched gate pulse inputs for the three bridges of the inverter are generated by the control system described below. The modulated pulse output of the inverter goes through an LCL filter to remove the higher order harmonics. Additionally, a RC snubber circuit is included to dampen out transients. Finally, a Δ-Y transformer is cascaded at the end.

The control system for the grid-tie inverter system operates by following the local frequency and outputting a desired amount of active power. To produce a stable grid frequency and phase measurement the control system uses the phase-locked loop (PLL) logic from the SimPowerSystems with automatic gain control. A SimPowerSystems discrete measurement block is used to sample P and Q every millisecond. These values are then compared to a setpoint and the error values are fed into an integral controller. The controller is implemented in the $dq0$ reference frame. The direct and quadrature axes correspond to active and reactive power generation, respectively. The integral action for each of these axes along with the frequency measurement from the PLL are used to generate a 3-phase signal that determines the switching pulses for the gates of the inverter. This control system uses the $dq0 \mapsto abc$ transformation block from the SimPowerSystems toolbox.

The sim runs on a computer with 2.4GHz dual-core Intel Core i5 processor and 4GB memory. Each simulation takes approximately 3 minutes, running with a discrete solver in rapid accelerator mode. Exhaustive simulations for all feasible combination of model parameters could provide a conclusion about the stability and performance for future distribution systems with different penetration of distributed generation. The sim has in excess of 20 parameters. Assuming a grid with 5 values for each parameter, the total simulation run time for the full parameter sweep would be $5^{20} \cdot 3$ min ≈ 0.5 Billion years! An alternative approach is discussed in the next section.

III. Surrogate Model

An approach of this study is to replace the described detailed simulation model with a much simpler surrogate model. The surrogate model is single-phase in circuits (while the power measurements are 3-phase); its blocks match the performance of the detailed model blocks. This allows us to characterize the closed loop. The surrogate model has fewer parameters and can be evaluated much faster than the detailed model. This makes exhaustive analysis possible.

The high-level systems diagram of the surrogate model is illustrated in Fig. 2. The Grid Interface Circuit receives inputs of the grid voltage V_G and the supplied inverter current I_N. The Inverter System output is I_N. At the input it computes instantaneous 3-phase active power output P_N and reactive Q_N through I_N and output voltage V_N. It also receives setpoints for the active P_{set} and reactive Q_{set} power. Note that V_G, V_N, and I_N are Root-Mean-Square (RMS) phasors.

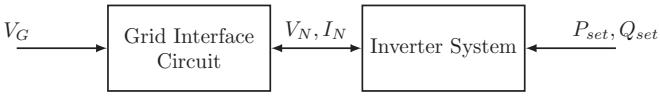

Fig. 2. High-level model of distribution system.

A. Grid Interface Circuit

The Grid Interface Circuit is the connection between the utility grid and the inverter. Its model is shown in Fig. 3, where Z_G is the impedance of the transmission lines and Z_L is the aggregated load impedance. The utility grid is modeled as a constant voltage source as seen by the distribution system. Since transmission line impedance scales linearly with distance, and the inverter is located much closer to the load than the utility grid, it was reasoned that the impedance between the inverter and the load could be neglected.

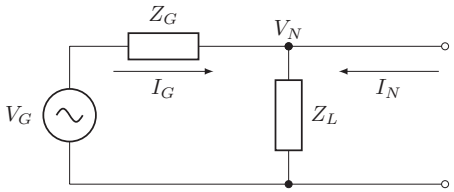

Fig. 3. Grid Interface Circuit.

B. Inverter Operation

A voltage difference between V_G and V_N causes current I_G to flow, delivering power from the grid to the load. The inverter acts as a current source with output I_N. The controller adjusts the output current of the inverter to reach the desired

power flow. The grid together with the inverter supply the 3-phase active P_L and reactive Q_L load power. The grid must supply the entirety of the reactive power to the load because grid-tie inverters are required to provide none.

C. Steady-State Analysis

This system will first be analyzed in steady-state. We assume the following grid parameters are given:

- distributed generation penetration: $a = 3V_N I_N^*/P_L$,
- power factor of the load: $\cos(\psi)$ with $\psi = \angle(P_L + iQ_L)$,
- magnitude of the load power: $|P_L + iQ_L|$,
- transmission line impedance: $Z_G = |Z_G|\angle\gamma$,
- magnitude of the utility grid voltage: $|V_G|$,

Note that we assume $P_{set} = aP_L$ and $Q_{set} = 0$ implicitly. We would like to solve for V_N and I_N.

Let $V_N = |V_N|\angle\phi$, $I_N = |I_N|\angle\phi$, $V_G = |V_G|\angle(\phi+\varphi)$, and $I_G = |I_G|\angle(\phi+\theta)$. Note that ϕ offsets all phasors and can be chosen arbitrarily. The steady-state solution must follow power flow equations and Ohm's law:

$$3V_N I_N^* = aP_L \tag{1}$$

$$3V_N I_G^* = (1-a)P_L + iQ_L \tag{2}$$

$$V_G = V_N + I_G Z_G \tag{3}$$

From (2), we have

$$\theta = \tan^{-1}\left(-\frac{Q_L}{(1-a)P_L}\right) \tag{4}$$

$$|I_G| = \frac{1}{3|V_N|}\sqrt{Q_L^2 + (1-a)^2 P_L^2} \tag{5}$$

Substituting (4) and (5) into (3) yields a biquadratic equation in $|V_N|$. It can be shown that when

$$|V_G|^2 \geq \frac{2}{3}|Z_G|(1+\cos(\theta+\gamma))\sqrt{Q_L^2 + (1-a)^2 P_L^2},$$

the equation has real roots, i.e. the steady-state exists. The solution is obtained as the largest of the four equation roots.

After $|V_N|$ is determined, $|I_N|$, $|I_G|$, and $|V_G|$ can be found from (1), (5), and (3), respectively. Finally, $P_L + iQ_L = 3\frac{|V_N|^2}{Z_L^*}$, yields the load impedance Z_L.

IV. Transient Analysis

To allow analysis of the system stability, the surrogate model includes the transients and the disturbances of the grid power that the distribution system should suppress. This section introduces a dynamic phasor model. The phasors are considered as functions of time that change much slower than AC oscillations. The analysis uses linearized models of the phasor variation dynamics in the vicinity of the steady state. The phasors in the model are $I_N + \delta I_N(t)$, $V_N + \delta V_N(t)$, and $V_G + \delta V_G(t)$, where $\delta I_N(t)$, $\delta V_N(t)$, and $\delta V_G(t)$ are the transient variations from the steady state solution of Section III-C. Although the magnitude of the grid voltage V_G is assumed to be constant, the grid frequency can be varying. Below, the time varying frequency is described through time-varying phasor V_G and is considered as an external disturbance.

In what follows, we develop transfer functions for the Grid Interface Circuit and the Inverter System block in Fig. 2.

A. Inverter System Overview

The Inverter System block includes the physical inverter, its control system, and all associated components. The Inverter System components are shown in Fig. 4 and include the PQ Measurement block, the PI Controllers block, the PLL block, the Phase Converter block, the Inverter Gain block, and the LCL Filter block. The transfer function of the Inverter System can be obtained by deriving the transfer functions of each individual component block. This is done below.

The goal of the inverter is to supply a specified amount of active and reactive power (P_{set} and Q_{set}) at the same frequency as the grid. The control system for the grid-tie inverter system follows the local frequency to output desired active and reactive power. A sensor measures active power (P) and reactive power (Q) at the output of the inverter. These values are then compared to a setpoint and the error values are fed into a PI controller. The setpoint for P could come from cascaded logic such as a MPPT algorithm. The setpoint for Q is assumed to be zero since grid-tie inverters, by regulation, are not allowed to inject reactive power. Additionally, a PLL is used to measure the frequency and phase at the grid connection point of the inverter. The control signals from the two PI controllers are used in conjunction with this frequency measurement to generate switching pulses for the gates of the inverter. The output current of the inverter is then fed through a low-pass LCL filter to remove higher harmonics and produce a clean signal at the desired frequency (60 Hz for the United States). This is combined with the power supplied by the utility grid to meet the load demand.

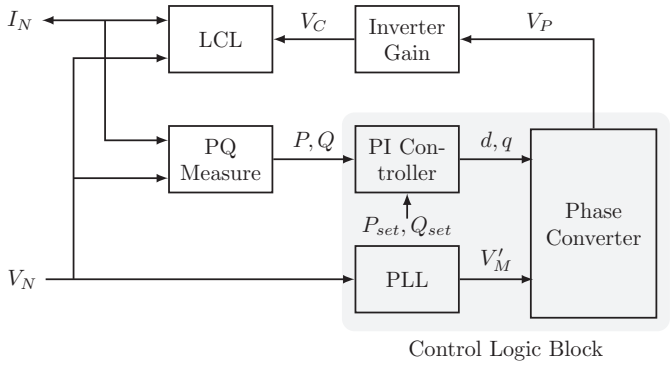

Fig. 4. Inverter system.

B. PQ Measurement

The 3-phase PQ Measurement block takes input current phasor I_N and voltage phasor V_N (each a 2-dimensional vector) and calculates active power $P = \Re(3V_N I_N^*)$ and $Q = \Im(3V_N I_N^*)$, where $\Re$ and $\Im$ denote the real and imaginary part of a complex variable respectively. This is assumed to be done with negligible delay. The linearized model of the block is then a static 2×4 gain matrix of the form

$$\begin{bmatrix}\delta P \\ \delta Q\end{bmatrix} = 3\begin{bmatrix}\Re I_N & \Im I_N & \Re V_N & \Im V_N \\ -\Im I_N & \Re I_N & \Im V_N & -\Re V_N\end{bmatrix}\begin{bmatrix}\Re\delta V_N \\ \Im\delta V_N \\ \Re\delta I_N \\ \Im\delta I_N\end{bmatrix}. \tag{6}$$

C. PI Controller

Two PI controller blocks feed the deviations of P and Q from the setpoints into PI controllers for the direct, d, and quadrature, q, control signals as shown in Fig. 5. In the steady state $P = P_{set}$ and $Q = Q_{set}$. Since the controller is linear, the model in variations has the same form as the control logic

$$\delta d = \left(K_d + \frac{K_{d_I}}{s}\right)(\delta P_{set} - \delta P), \tag{7}$$

$$\delta q = \left(K_q + \frac{K_{q_I}}{s}\right)(\delta Q_{set} - \delta Q), \tag{8}$$

where s is the Laplace operator, K_d, K_{d_I}, K_q, and K_{q_I} are the controller constants, δP, δQ are the outputs in (6), and δP_{set}, δQ_{set} are the external command inputs.

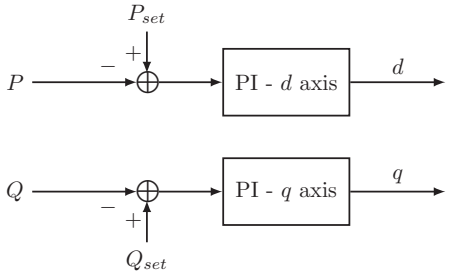

Fig. 5. PI controller blocks.

D. PLL

The PLL block measures phase from the input V_N and generates output V'_N with unit amplitude. Let the input be $V_N = |V_N|\angle\theta_i$ and the output $V'_N = 1\angle\theta_o$. At steady-state, the amplitude of input is a constant $|V_N|$, the output phase $\theta_o = \theta_i$, and the output frequency is the constant $f_o = \frac{1}{2\pi}\frac{d}{dt}\theta_o$.

Linearizing $\theta_i = \tan^{-1}(\Im(V_N)/\Re(V_N))$ for a transient perturbation δV_N, we get

$$\delta\theta_i = \frac{1}{|V_N|^2}\begin{bmatrix}-\Im V_N & \Re V_N\end{bmatrix}\begin{bmatrix}\Re\delta V_N \\ \Im\delta V_N\end{bmatrix}. \tag{9}$$

The PLL uses PI feedback of the tracking error with the transfer function $2\zeta_p w_p + w_p^2/s$. Then, according to [9],

$$\delta\theta_o = \frac{2\zeta_p w_p s + w_p^2}{s^2 + 2\zeta_p w_p s + w_p^2}\delta\theta_i. \tag{10}$$

Finally, given that $V'_N = 1\angle\theta_o = \cos(\theta_o) + i\sin(\theta_o)$ and $\theta_o = \theta_i$ at steady-state, we have

$$\begin{bmatrix}\Re\delta V'_N \\ \Im\delta V'_N\end{bmatrix} = \begin{bmatrix}-\sin(\theta_o) \\ \cos(\theta_o)\end{bmatrix}\delta\theta_o = \frac{1}{|V_N|}\begin{bmatrix}-\Im V_N \\ \Re V_N\end{bmatrix}\delta\theta_o. \tag{11}$$

Combining (9), (10), and (11) yields the transient map from δV_N to $\delta V'_N$.

E. Phase Converter

The Phase Converter block receives the inputs of d, q (from the PI controller), and V'_N (from the PLL), and produces the phasor V_P that drives the switching of the gates of the inverter to produce the desired current. The converter takes the instantaneous phase of the input phasor V'_N and modulates it with the amplitude d. It also adds a quadrature signal with amplitude q. This can be expressed as

$$V_P = \frac{1}{\sqrt{2}}(d + iq)V'_N, \tag{12}$$

where the scale $\frac{1}{\sqrt{2}}$ ensures that V_P is a RMS measurement. Nonlinear model (12) has 4 inputs (two components of V'_N, d, and q) and 2 outputs. The model in variations obtained by linearizing (12) has the form

$$\begin{bmatrix}\Re\delta V_P \\ \Im\delta V_P\end{bmatrix} = \frac{1}{\sqrt{2}}\begin{bmatrix}d & -q & \Re V'_N & -\Im V'_N \\ q & d & \Im V'_N & \Re V'_N\end{bmatrix}\begin{bmatrix}\Re\delta V'_N \\ \Im\delta V'_N \\ \delta d \\ \delta q\end{bmatrix},$$

where δd and δq are the outputs in (7) and (8).

F. Inverter Gain

The output of the inverter is the signal $V_C = K_{inv}V_P$, where gain K_{inv} is determined by the DC side of the inverter. Thus, the model for the variation of δV_P is

$$\delta V_C = K_{inv}\delta V_P$$

G. LCL Filter

The final block is the LCL Filter. The switching action of the gates of the inverter generates high-frequency harmonics in the output signal. The LCL filter is used to remove these harmonics without the losses that would be caused by the impedance of a RC filter. The LCL filter in the simulation model was designed according to the guidelines in [4]. A Δ-Y transformer is usually cascaded at the end for any possible single phase connection. Our model lumps the transformer inductance with the LCL filter and includes a Δ-Y transformer with a unity gain. The equivalent circuit is shown in Fig. 6.

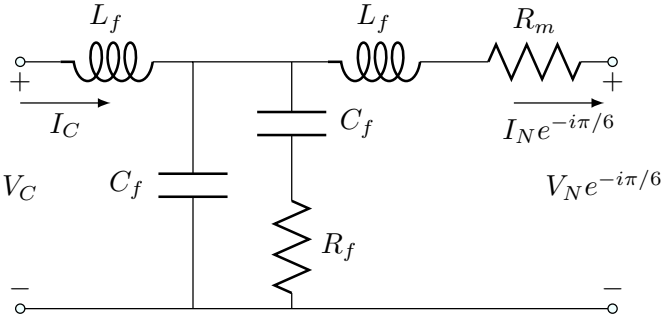

Fig. 6. LCL filter block.

This is a two-port network with a linear transfer function. Let Z_d be the load impedance. In steady-state, the linear transfer function T_{lcl} from V_C to I_N can be derived using $Z_d = V_N/I_N$. In a transient, $Z_d = Z_L||Z_G$ ($||$ denotes the parallel connection), and the map from δV_C to δI_N is given by phasor transfer function $T_{lcl}(s + iw_0)$ with $w_0 = 2\pi f_0$ (where f_0 = 60 Hz in the US).

H. Transient Grid Inverter Circuit

The disturbance δV_G propagates to the inverter through the Grid Interface Circuit as follows,

$$\delta V_N = \frac{Z_L||Z_N}{Z_G + (Z_L||Z_N)}\delta V_G + (Z_G||Z_L)T_{lcl}(s+iw_0)\delta V_C, \tag{13}$$

$$\delta I_N = -\frac{Z_L||Z_N}{Z_G + (Z_L||Z_N)}\frac{1}{Z_N}\delta V_G + T_{lcl}(s+iw_0)\delta V_C, \tag{14}$$

where Z_N is the output impedance of the inverter, which is equivalent to

$$Z_N = (T_{lcl}(s+iw_0))^{-1}\big|_{V_C=0}.$$

Note that (13) and (14) are consistent with the linearized map defined by the circuit in Fig. 3

$$\delta V_N = \frac{Z_L}{Z_G + Z_L}\delta V_G + (Z_G||Z_L)\delta I_N.$$

However, we cannot treat δI_N as an ideal current source and must also take the inverter impedance Z_N into consideration.

I. Frequency Disturbance Analysis

In this section we derive the relationship between a change in the grid phase and the corresponding change in the inverter voltage V_N. Consider disturbance input V_G in the Grid Interface Circuit model. We assume that the grid voltage magnitude is constant but the frequency is changing. The grid frequency variation is modeled as phase variation.

Suppose $V_G = |V_G|e^{i\Phi_{V_G}}$ and there is a phase change $\delta\Phi_{V_G}$ in V_G due to a frequency disturbance $\delta\omega_{V_G} = \frac{d}{dt}\delta\Phi_{V_G}$. To reflect the time varying phase $\delta\Phi_{V_G}$ the steady state phasor V_G is replaced by the time-varying phasor $V_G + \delta V_G$ by

$$\delta V_G = |V_G|e^{i\Phi_{V_G}} i\delta\Phi_{V_G} = V_G i\delta\Phi_{V_G}.$$

This yields the disturbance input phasor δV_G in (13) and (14)

$$\begin{bmatrix}\Re\delta V_G \\ \Im\delta V_G\end{bmatrix} = \begin{bmatrix}\Re V_G & -\Im V_G \\ \Im V_G & \Re V_G\end{bmatrix}\begin{bmatrix}0\\1\end{bmatrix}\delta\Phi_{V_G}.$$

The phase change $\delta\Phi_{V_N}$ in V_N caused by δV_N can be determined by linearizing the steady-state map

$$\Phi_{V_N} = \tan^{-1}\left(\frac{\Im V_N}{\Re V_N}\right)$$

to yield the disturbance of the inverter voltage phase

$$\delta\Phi_{V_N} = \frac{1}{|V_N|^2}\begin{bmatrix}-\Im V_N & \Re V_N\end{bmatrix}\begin{bmatrix}\Re\delta V_N \\ \Im\delta V_N\end{bmatrix}.$$

Note that the transfer function from $\delta\omega_{V_G}$ to $\delta\omega_{V_N} = \frac{d}{dt}\delta\Phi_{V_N}$ is the same as that from $\delta\Phi_{V_G}$ to $\delta\Phi_{V_N}$ since

$$\frac{\delta\omega_{V_N}}{\delta\omega_{V_G}} = \frac{s\delta\Phi_{V_N}}{s\delta\Phi_{V_G}} = \frac{\delta\Phi_{V_N}}{\delta\Phi_{V_G}}.$$

V. Transient Analysis Results

The surrogate model was verified by comparing it to the detailed simulation model. First, verification tests were performed for various parameters to ensure that each block of the surrogate model and the respective part of the detailed simulation model have very similar responses. Then, the complete closed loop models integrated from the verified blocks were matched. Fig. 7 shows the responses to a step in the active power of the inverter P_{set} and the reactive power Q_{set} for both the surrogate model and the detailed simulation. These responses match reasonably well. The developed surrogate model is a good approximation of the detailed simulation and the results below should be applicable to a range of real distribution systems. The goal of the transient analysis

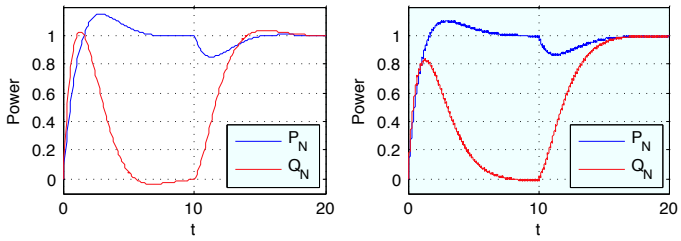

Fig. 7. Step responses of P_{set} (at $t = 0$) and Q_{set} (at $t = 10$) for the surrogate model (left) and the detailed simulation (right).

is to determine how the system responds to a disturbance in the phase of the utility grid. Equations in Section IV were combined to develop a complete transfer function relating the disturbance input $\delta\omega_{V_G}$ to the output $\delta\omega_{V_N}$. We explored the model parameters to determine where the distribution system can be guaranteed to stably operate despite disturbances from the grid. Each block in the surrogate model developed previously was coded in MATLAB and connected into the full system using the Control System Toolbox. This allowed for the development of a complete transfer function from a grid phase disturbance to the measured phase of the distribution system. The analysis covered a range of model parameters as shown in Table I.

In accordance with [10], the impedance of the low voltage line was calculated as $Z_L = (0.642{+}i0.083)l\ \Omega$, where l is the line length in km shown in Table I. We only need to consider the low-voltage line, since the equivalent impedance of the mid-voltage and high-voltage lines is comparatively small.

For the PLL model (10), the analysis used $\zeta_p \in [0.3, 0.65]$ and $w_p \in [11, 57]$. Table I describes the PLL through rise time, which is proportional to w_p^{-1}, and overshoot, which is defined by the damping factor ζ_p.

For the LCL filter, we analyzed $R_f \in [0.1, 0.8]$, and $L_f \in [5{\cdot}10^{-3}, 5{\cdot}10^{-2}]$, see Fig. 6. We assume transformer resistance $R_m = 0.007$ to be a fixed parameter. Table I describes the LCL filter through power loss and settling time parameters. The power loss increases with the resistance R_f, which also reduces the Q-factor at the resonance and helps stability. The settling time increases with L_f. To maintain the LCL filter resonance frequency, we kept $L_f C_f = 5 \cdot 10^{-7}$, see [4].

The system has a stable step response over all explored parameter values. It is a somewhat surprising result that the

TABLE I
SURROGATE MODEL PARAMETER SWEEP

Parameters	Minimum Value	Maximum Value
Penetration a	0.05	0.95
Load power P_L	5kW	40kW
Power factor $\cos(\psi)$	0.9	1.00
Line length l	25m	1km
PLL rise time	0.02s	0.1s
PLL overshoot	23%	45%
LCL power loss	3×0.024Watts	3×16.3Watts
LCL settling time	2.04s	19.5s

system performs well under all reasonable operating conditions. This shows that it is possible, with reasonably tuned PI controllers, to build a very stable system.

For each combination of these parameters, the H_∞ norm of the closed-loop transfer function from $\delta\omega_{V_G}$ to $\delta\omega_{V_N}$ was calculated for the resultant transfer function. The H_∞ norm shows the maximum gain by which the frequency variation is amplified at any frequency of the disturbance. Overall 25,000 combinations of the system parameters were explored. With about 1s per run this took about 7 hours. The results shows that the H_∞ norm is always less than 1.61 for all sample points we considered and is less than 1.2 if line length $l < 0.5$km.

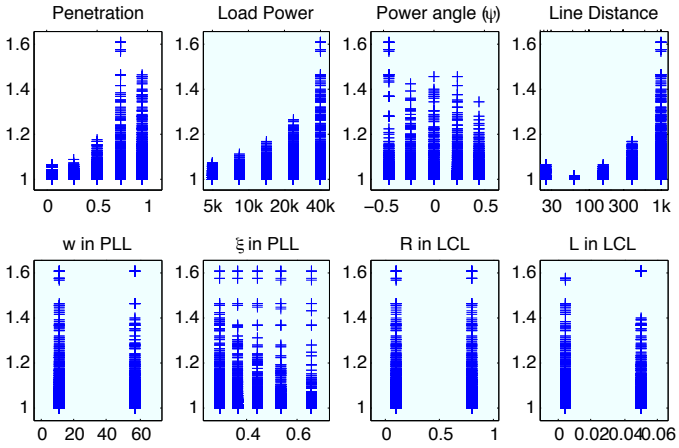

Fig. 8. Transient analysis results: the H_∞ norm vs each parameter in Table I. At each sample value of the parameter, the markers show the values of the H_∞ norm for all analyzed combinations of other parameters.

In all simulations the PI controller (7) and (8) used the I (integral) gains $K_{d_I} = 2.25 \cdot 10^{-4}$ Volt/(Watt·s) in the direct (active power P) control channel (7) and $K_{q_I} = -3 \cdot 10^{-5}$ Volt/(Watt·s) in the quadrature (reactive power Q) control channel (8). The P (proportional) controller gains were set to zero. The controller gains were initially tuned using Simulink Control System Toolbox tools over a coarse grid of K_{d_I} and K_{q_I}. This required building the surrogate model as a Simulink block diagram. Building the alternative Simulink version of the surrogate model provided an additional method to verify that it was integrated correctly.

The same fixed controller tuning was used in all of the analysis runs. This controller tuning could be, and likely is, suboptimal for many of the system parameter sets explored. The fixed tuning corresponds to a real-world scenario, where the controller comes with the inverter box and is not retuned for different installations where grid parameters vary. The results obtained show that the system is stable and the disturbance amplification is not unreasonably large for such suboptimal controller. A better tuning of the controller might further reduce the disturbance amplification but would not change the conclusions.

VI. CONCLUSION

A grid-connected distribution system with an aggregated load and inverter-connected distributed generation was analyzed. The system was broken into its component blocks and linearized models (transfer functions) were developed for each of these blocks. A transient analysis shows that the system has a stable response and no excessive amplification of grid frequency disturbances. These results are obtained over a full exploration of the parameter space. Based on the model studied, the distribution system has no frequency stability issues for all reasonable operating parameters even with high penetration of inverter-connected generation. The lack of rotating inertia does not seem to be a limiting factor.

These results are applicable only if the system parameters allow an acceptable steady state solution. One of the reasons why such solution might be unavailable is related to the active power supply. Due to regulation, a grid-tie inverter can only supply power at unity power factor. Therefore, as the inverter supplies a larger percentage of the load, the power factor of the distribution system as seen by the grid will necessarily decrease as long as there is any reactive component to the load. Typically any power factor above 0.9 is acceptable to a utility, although this varies based on local regulations. In cases such as this, power factor restrictions might define the practical limits of inverter penetration.

REFERENCES

[1] J. Smith, W. Sunderman, R. Dugan, and B. Seal, "Smart inverter volt/var control functions for high penetration of pv on distribution systems," in *IEEE Power Systems Conference and Exposition (PSCE)*, 2011.

[2] R. Tonkoski, L. Lopes, and T. El-Fouly, "Coordinated active power curtailment of grid connected pv inverters for overvoltage prevention," *IEEE Trans. on Sustainable Energy*, vol. 2, no. 2, pp. 139–147, 2011.

[3] *Interconnecting Distributed Resources with Electric Power Systems*, IEEE Std. 1547, 2003.

[4] P. Channegowda and V. John, "Filter optimization for grid interactive voltage source inverters," *IEEE Trans. on Industrial Electronics*, vol. 57, no. 12, pp. 4106–4114, 2010.

[5] I. Gabe, V. Montagner, and H. Pinheiro, "Design and implementation of a robust current controller for vsi connected to the grid through an lcl filter," *IEEE Trans. on Power Electronics*, vol. 24, no. 6, pp. 1444–1452, 2009.

[6] C.-L. Chen, J.-S. Lai, Y.-B. Wang, S.-Y. Park, and H. Miwa, "Design and control for lcl-based inverters with both grid-tie and standalone parallel operations," in *IEEE Industry Applications Society Annual Meeting*, 2008.

[7] J. Morren, S. de Haan, and J. Ferreira, "Primary power/frequency control with wind turbines and fuel cells," in *IEEE Power Engineering Society General Meeting*, 2006.

[8] Mathworks. (2011) Recorded webinar: Modeling and simulation of pv solar power inverters. [Online]. Available: http://www.mathworks.com/wbnr57525

[9] T. C. Wang, S. Lall, and T. Y. Chiou., "Polynomial method for pll controller optimization," *Sensors*, vol. 11, no. 7, pp. 6575–6592, 2011.

[10] A. Engler and N. Soultanis, "Droop control in lv-grids," in *International Conference on Future Power Systems*, 2005.